Joint Beamforming for Secure Communication in RIS-Assisted Cognitive Radio Networks

Xuewen Wu, Jingxiao Ma, and Xiaoping Xue

***Abstract*—This paper studies the security and communication efficiency problem of a reconfigurable intelligent surface (RIS) assisted cognitive radio network, in which we proposed a scheme where secrecy rate (SR) and transmission rate are jointly considered. In specific, with the help of RIS, we exploit the green interference caused by the secondary network to ensure the physical layer security of the primary network. By taking the mutual interference between these two networks into account, we establish a problem to minimize the total transmit power subject to the quality-of-service requirement of secondary user (SU), SR requirement of the primary users (PUs) and limited interference temperature of PUs. In our proposed iterative algorithm, the transmit and reflect beamforming are alternatively optimized by transforming PUs' SR constraint into a second order cone (SOC) form, and the optimal transmit and reflect beamforming are achieved based on the iterative penalty function. Simulation results show the superiority of our proposed algorithm in terms of the total transmit power requirement compared with other benchmarks, and the total transmit power of our proposed algorithm is not very susceptible to the number of eavesdroppers and PUs, which is conducive to serving multiple users in the wireless communication system.**

***Index Terms*—Cognitive radio network, green interference, physical layer security, reconfigurable intelligent surface, secrecy rate.**

I. Introduction

In the past decades, new wireless communication systems have grown exponentially, resulting in the shortage of spectrum. To this end, cognitive radio networks (CRN) was proposed as a promising technology to improve the spectrum efficiency (SE) [1], which can alleviate the scarcity of spectrum. In the CRNs, there exists two kinds of users, namely primary user (PU) and secondary user (SU), where the SU adopts the spectrum authorized to the PU for communication under the premise that SU will not cause significant interference to PU [2]. Therefore, two spectrum access methods have been proposed, namely opportunistic spectrum access and spectrum underlay. For opportunistic spectrum access, SUs detect the spectrum holes of PU and use them to support their own transmission. The fatal defect of such scheme is that the identification of spectrum holes should be very precise, otherwise the communication of PU may be severely affected. For spectrum underlay access, SU is allowed to access PU's authorized spectrum simultaneously under the premise that the interference is within a predefined threshold [3], which can help guarantee PU's performance. Owes to the simple sensing mechanisms and control functions, the spectrum underlay method has attracted great attention [4]. To this end, we focus on the CRNs with spectrum underlay access in this paper.

However, in the underlay method, there is a contradiction between the performance improvements of PU and SU. On the other hand, the inherent broadcast characteristics of wireless communications make the security issue non-ignorable. In the underlay CRNs, SUs keep sensing PUs' transmission and adjust the transmit power to guarantee the communication of PUs [5]. Hence, when there exist eavesdroppers (Eves) in the transmission area of SUs or PUs, wiretapping may cause severe security issues. It is necessary to protect CRNs from eavesdropping. Some physical layer security (PLS) technologies have arisen to provide perfect security for data transmission. Due to the random characteristic of the wireless channel, there exists difference between the wiretap link and legitimate link, defined as the secrecy rate (SR) [6], which can be exploited to realize the secure communication. In particular, multi-antennas at the cognitive base station (CBS) were adopted in [7] to make SU's SR at its maximum under the premise of limited interference. In [8], cooperation between the secondary network (SN) and primary network (PN) was proposed to enhance PN's secrecy capacity. The authors of [9] investigated transmission techniques for a fundamental cooperative CRN to offer performance improvement of PU transmission. Interference is generally considered harmful in communication systems. However, interference can be appropriately exploited to improve the secrecy performance [10]–[15]. A joint beamforming for signal and artificial noise was proposed in [10] to ensure the secure communication of PN and SN. Based on the nullspace of the legitimate channel, a jamming beamforming scheme was exploited in [11] to protect the primary system. With the aid of artificial noise (AN) to jam the Eves, the authors of [12] proposed a cooperative method to maximize the SR of SN subject to PUs' SR constraints. In [13], as a friendly jammer, the unmanned aerial vehicle (UAV) can enhance SU's secrecy performance by jointly optimizing the power and trajectory of UAV in the CRNs. Also, [14] and [15] studied an UAV-assisted jamming CRN to improve the secrecy performance of PN and SN, respectively.

Nevertheless, [10]–[15] have to consume additional power to exploit the interference. In fact, there exists mutual interference between the PN and SN of the CRN itself. In

Manuscript received April 12, 2022 revised August 11, 2022; approved for publication by Qingqing Wu, Guest Editor, October 4, 2022.

This work was supported by National Natural Science Foundation of China under Grant 61871290, Shanghai Science and Technology Innovation Action Plan under Grant 21DZ1200702. (*Corresponding author: Jingxiao Ma.*)

The authors are with the College of Electronic and Information Engineering, Tongji University, Shanghai 201804, China. email: wuxuewen1995@163.com, {mjxiao, xuexp}@tongji.edu.cn.

J. Ma is the corresponding author.

Digital Object Identifier: 10.23919/JCN.2022.000044

this paper, we are interested in the security problem of PN. The interference from the secondary transmitter is adopted as a useful resource to improve the secrecy performance of PN [16]–[18]. However, a relatively large number of CBS antennas are required to achieve good performance, which in turn leads to high hardware complexity and cost.

A good solution to the problems mention above is to introduce a reconfigurable intelligent surface (RIS) into the CRNs. Recently, as a result of full-duplex transmission and low power consumption, RIS has become a promising technology to significantly increase the SE in wireless communications [19]. It is cost-effective and energy-saving, which is able to shape wireless channel environment and can play an important role in the scenario that direct links are unavailable [20]. Different from the traditional active relays and transceivers, RIS adopts passive structure to reflect incident signal without any complex signal processing and power amplification, and has no extra power consumption [21]. The existing contributions have illustrated the advantages of introducing RIS into various communication networks. Specifically, by properly designing the beamforming at the access point (AP) and RIS, transmission rate or received signal power [22]–[28], SR [29]–[34], transmit power [35]–[37], and energy efficiency [38] can be obtained at the optimal value.

Until now, only a few studies have focused on the joint beamforming design in the RIS-assisted CRNs. In [39], considering an RIS-assisted CRN coexisting with a PN, the authors investigated the transmit power minimization problem through designing the joint beamforming at the SU transmitter and RIS. Considering the statistical channel state information (CSI) error model of PU links, the authors of [40] studied the power minimization problem via robust beamforming design in RIS-assisted CRNs. In addition to the power minimization problem, the SU transmission rate maximization problem in the RIS-assisted CRNs has also been investigated in [41]–[43]. The works mentioned above did not consider the security issue. Considering the trade-off between SR and energy consumption, [44] investigated the secrecy energy efficiency (SEE) maximization problem via joint beamforming at the CBS and RIS, where the secure transmission design was based on perfect CSI of Eves, which is hard to be attained in practice. As such, assuming that imperfect CSIs of angle-of-departures for wiretap links are known, an optimization problem to maximize the worst-case achievable SR of SU was formulated in [45]. Considering different cases of Eve's CSI, the authors of [46] proposed a PLS scheme to enhance the SR of SU in the RIS-assisted CRNs. It should be noted that [44], [46] which studied the RIS-assisted CRNs focused on improving the secrecy performance of SU, and ignored the mutual interference of the two networks and the performance of PN. To our best knowledge, no related works have studied the joint beamforming design of CBS and primary base station (PBS) in the RIS-assisted CRNs yet. This observation motivates us to propose a joint beamforming scheme to ensure the transmission of SU while enhancing the PLS of PN by properly exploiting the green interference from the SN. In summary, our main contributions are listed as follows:

TABLE I
NOTATION SUMMARY.

Symbol	Representation
$\|\cdot\|$	The Euclidean norm of a vector
$\mathrm{diag}(\mathbf{x})$	The diagonal matrix with $\mathbf{x}$ on its main diagonal
$\|\mathbf{X}\|$	The determinant of matrix $\mathbf{X}$
$C^{M\times N}$	The complex space of $M \times N$
$\mathrm{tr}(\mathbf{X})$	The trace of matrix $\mathbf{X}$
$\lambda_{\max}(\mathbf{X})$	The maximum eigenvalue of matrix $\mathbf{X}$
$\mathbf{I}_M$	The $M \times M$ identity matrix
$\mathbf{a} \otimes \mathbf{b}$	The Kronecker product of $\mathbf{a}$ and $\mathbf{b}$
$[\mathbf{X}]_{i,j}$	The (i,j)th element of $\mathbf{X}$
$(\cdot)^T$	The transpose operation
$\mathbf{X} \succeq 0$	$\mathbf{X}$ is a positive semi-definite matrix
$(\cdot)^H$	The Hermitian transpose operation
$\langle \mathbf{X}, \mathbf{Y} \rangle$	$\mathrm{tr}\left(\mathbf{X}^H \mathbf{Y}\right)$
$\|\cdot\|$	The absolute value
$\log_2(\cdot)$	The logarithmic function
$\mathrm{rank}(\mathbf{X})$	The rank of matrix $\mathbf{X}$
$E[\cdot]$	The expectation operator

- We propose a new RIS-assisted CRN framework with software defined architecture (SDA), by which the control plane attains and adopts the global knowledge, including quality of service (QoS) requirements and CSIs, to realize the resource allocation and dynamic reconfiguration, thereby reducing user plane's signaling overhead. Our framework provides the probability to jointly design the beamforming for the RIS-assisted CRNs, so as to enable the PN and SN cooperate with each other.
- By taking the mutual interference between the PN and SN into account, we establish a constrained problem to minimize the total transmit power. To our best knowledge, this is the first research on studying such an optimization design where the RIS not only plays a role in improving the SE of SU, but also enhances the secrecy performance of PUs by generating green interference to PN with a high degree of freedom in an energy-saving way.
- In our proposed iterative algorithm, the transmit and reflect beamforming are alternatively optimized by transforming PUs' SR constraint into a second order cone (SOC) form and solved with introduction of an iterative penalty function. Simulation results show the superiority of our proposed algorithm and the total transmit power of the proposed algorithm is not very susceptible to the number of Eves and PUs, which is beneficial for the next generation mobile communication to serve multiple users.

The rest of this paper is organized as follows. Section II introduces the system model followed by problem formulation, which is solved in Section III. Simulation results are presented in Section IV. Finally, Section V concludes the paper.

For convenience, Table I shows a list of symbols included in this paper.

II. System Model and Problem Formulation

As shown in Fig. 1, consider a SDA-based-RIS-assisted downlink CRN comprising software components to decouple the control and user plane to provide flexibility and swiftness,

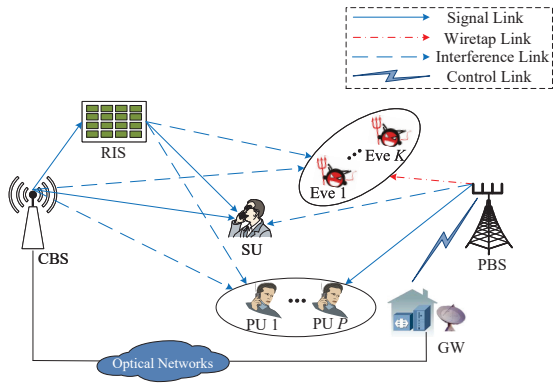

Fig. 1. A SDA-based-RIS-assisted downlink CRN with a CBS, a SU sharing the spectrum with P PUs served by a PBS.

in which SU uses the spectrum with P PUs served by the PBS. The gateway manages the resource allocation to enable the PN cooperative with the SN as a control center. Specifically, in the PN, a M_p-antenna PBS serves P PUs, and the PBS–PUs transmission will be wiretapped by K Eves. In the SN, a CBS equipped with M_c antennas uses the spectrum allocated to PUs to establish communication with a single-antenna SU by means of an RIS. In this paper, to enhance SU's received signal strength and exploit green interference generated by the SN to increase the security of PN in an energy-saving manner, a RIS having N passive elements is exploited. Thanks to the large path loss, the power of signals reflected multiple times is negligible [42]. Supposing the scenario that the Eves are active users yet untrusted by the legitimate user, the CSIs of the wiretap links can be obtained [33], [47]. By assuming that all involved channels subject to quasi-static flat-fading and perfect CSIs of all links are available at the gateway, we are meant to design a joint beamforming scheme to make the transmit power at its minimum value, under the premise that the QoS of SU, the SRs of PUs, the interference temperature of PUs and the modulus of RIS meet corresponding constraints.

Assume that PBS exploits the linear transmit precoding, i.e., an independent transmit beamforming vector $\mathbf{w}_p \in C^{M_p \times 1}$ is adopted for every PU. To this end, the transmission signal at the PBS can be written as $\mathbf{x} = \sum_{p=1}^{P} \mathbf{w}_p x_p$, in which x_p stands for the transmit symbol for the pth PU satisfying $E\left[|x_p|^2\right] = 1$. As such, the transmit power budget at the PBS can be given by

$$P_{PBS} \geq \sum_{p=1}^{P} \|\mathbf{w}_p\|^2. \tag{1}$$

At the same time, CBS transmits the signal s satisfying $E\left[|s|^2\right] = 1$ to SU via RIS with transmit beamforming vector $\mathbf{v} \in C^{M_c \times 1}$. Owing to the shared radio spectrum of PN and SN, the received signals at the SU, pth PU and kth Eve that wiretaps the pth PU can be, respectively, given by

$$y_s = \left(\mathbf{h}_s^H \mathbf{Q}\mathbf{H} + \mathbf{h}_{ds}^H\right)\mathbf{v}s + \mathbf{f}_s^H \sum_{p=1}^{P} \mathbf{w}_p x_p + n_s, \tag{2a}$$

$$y_p = \underbrace{\mathbf{f}_p^H \mathbf{w}_p x_p}_{\text{desired signal}} + \underbrace{\mathbf{f}_p^H \sum_{i=1, i\neq p}^{P} \mathbf{w}_i x_i}_{\text{inter-user interference}} + \underbrace{\left(\mathbf{h}_p^H \mathbf{Q}\mathbf{H} + \mathbf{h}_{dp}^H\right)\mathbf{v}s}_{\text{interference from SN}} + \underbrace{n_p}_{\text{noise}}, \quad \forall p, \tag{2b}$$

$$y_{k,p} = \underbrace{\mathbf{f}_{e,k}^H \mathbf{w}_p x_p}_{\text{desired signal}} + \underbrace{\mathbf{f}_{e,k}^H \sum_{i=1, i\neq p}^{P} \mathbf{w}_i x_i}_{\text{inter-user interference}} + \underbrace{\left(\mathbf{h}_{e,k}^H \mathbf{Q}\mathbf{H} + \mathbf{h}_{de,k}^H\right)\mathbf{v}s}_{\text{interference from SN}} + \underbrace{n_{e,k}}_{\text{noise}}, \quad \forall k, p, \tag{2c}$$

where $\mathbf{H} \in \mathcal{C}^{N \times M_c}$ denotes the channel matrix of the CBS-RIS link. $\{\mathbf{h}_s, \mathbf{h}_p, \mathbf{h}_{e,k}\} \in \mathcal{C}^{N \times 1}$ are the channel vectors of the RIS to SU, pth PU and kth Eve links[1], respectively. $\left\{\mathbf{h}_{ds}, \mathbf{h}_{dp}, \mathbf{h}_{de,k}\right\} \in \mathcal{C}^{M_c \times 1}$ represent the channel vectors of the direct links from CBS to SU, pth PU and kth Eve, respectively. $\{\mathbf{f}_s, \mathbf{f}_p, \mathbf{f}_{e,k}\} \in \mathcal{C}^{M_p \times 1}$ are the channel vectors of the PBS to SU, pth PU and kth Eve links, respectively. $\mathbf{Q} = \text{diag}\left(a_1 e^{j\phi_1}, \cdots, a_n e^{j\phi_n}, \cdots, a_N e^{j\phi_N}\right)$, in which a_n and ϕ_n respectively represent the amplitude and phase shift of the nth reflecting element. For simplicity, we set $a_n = 1, \forall n$ [24]. n_s, n_p, and $n_{e,k}$ are the additive complex white Guassian noises at the SU, pth PU, and kth Eve, where the entries are with zero-mean and variance σ_v^2, $v \in \{s, p, \{e, k\}\}$. Following (2), the signal-to-interference-plus-noise ratio (SINR) at the SU, pth PU and kth Eve can be, respectively, expressed as

$$\gamma_s = \frac{\left|\mathbf{q}^H \mathbf{H}_s \mathbf{v}\right|^2}{\sum_{p=1}^{P} \left|\mathbf{f}_s^H \mathbf{w}_p\right|^2 + \sigma_s^2}, \tag{3a}$$

$$\gamma_p = \frac{\left|\mathbf{f}_p^H \mathbf{w}_p\right|^2}{\sum_{i=1, i\neq p}^{P} \left|\mathbf{f}_p^H \mathbf{w}_i\right|^2 + \left|\mathbf{q}^H \mathbf{H}_p \mathbf{v}\right|^2 + \sigma_p^2}, \forall p, \tag{3b}$$

$$\gamma_{k,p} = \frac{\left|\mathbf{f}_{e,k}^H \mathbf{w}_p\right|^2}{\sum_{i=1, i\neq p}^{P} \left|\mathbf{f}_{e,k}^H \mathbf{w}_i\right|^2 + \left|\mathbf{q}^H \mathbf{H}_{e,k} \mathbf{v}\right|^2 + \sigma_{e,k}^2}, \forall k, p, \tag{3c}$$

where $\mathbf{H}_v \triangleq \begin{bmatrix} \text{diag}\left(\mathbf{h}_v^H\right)\mathbf{H} \\ \mathbf{h}_{dv}^H \end{bmatrix}, v \in \{s, p, \{e, k\}\}$ represent the related channels of the SU, pth PU, kth Eve, respectively, which include both the cascade channel and direct channel. $\mathbf{q} \triangleq \left[e^{j\phi_1}, e^{j\phi_2}, \cdots, e^{j\phi_N}, 1\right]^H$.

As a result, SU's transmission rate and the pth PU's SR wiretapped by the kth Eve can be, respectively, written as

$$R_s = \log_2\left(1 + \gamma_s\right), \tag{4a}$$

[1]Usually, there are two main methods for the RIS involved channel acquisition, relying on whether the RIS elements are equipped with receive RF chains or not [24]. For the first method with receive RF chains, conventional channel estimation methods can be applied for the RIS to estimate the channels of the CBS-RIS and RIS-user links, respectively. For the second method without receive RF chains at the RIS, the RIS reflection patterns can be designed together with the uplink pilots to estimate the cascaded CBS-RIS-user channels [48], [49]. The proposed beamforming designs in this paper are applicable with both the above channel estimation methods.

$$\left[\mathrm{tr}\left(\mathbf{F}_p\mathbf{W}_p\right)+\left(1-2^{\Lambda_p^{\mathrm{sec}}}\right)\left(\mathrm{tr}\left(\mathbf{F}_p\mathbf{\Sigma}_p\right)+\mathrm{tr}\left(\mathbf{H}_p^H\mathbf{\Theta}\mathbf{H}_p\mathbf{V}\right)+\sigma_p^2\right)\right] \times\left[\mathrm{tr}\left(\mathbf{F}_{e,k}\mathbf{\Sigma}_p\right)+\mathrm{tr}\left(\mathbf{H}_{e,k}^H\mathbf{\Theta}\mathbf{H}_{e,k}\mathbf{V}\right)+\sigma_{e,k}^2+\frac{2^{\Lambda_p^{\mathrm{sec}}}}{2^{\Lambda_p^{\mathrm{sec}}}-1}\mathrm{tr}\left(\mathbf{F}_{e,k}\mathbf{W}_p\right)\right]\geq\frac{2^{\Lambda_p^{\mathrm{sec}}}}{2^{\Lambda_p^{\mathrm{sec}}}-1}\mathrm{tr}\left(\mathbf{F}_p\mathbf{W}_p\right)\mathrm{tr}\left(\mathbf{F}_{e,k}\mathbf{W}_p\right) \tag{10}$$

$$R_{k,p}^{\mathrm{sec}}=\log_2\left(1+\gamma_p\right)-\log_2\left(1+\gamma_{k,p}\right). \tag{4b}$$

To ensure the transmission of SU while enhancing the PLS of PN, we proposed a joint beamforming design that aims at making the transmit power reach its minimum while guaranteeing certain QoS of SU, achieving certain level of SR for the PUs and limiting the interference temperature of PUs, which can be mathematically written as a constrained optimization problem

$$\begin{aligned}\min_{\mathbf{w}_p,\mathbf{v},\mathbf{q}}\quad&\sum_{p=1}^{P}\|\mathbf{w}_p\|^2+\|\mathbf{v}\|^2 &(5a)\\ \text{s.t.}\quad&R_s\geq\Lambda_s, &(5b)\\ &R_{k,p}^{\mathrm{sec}}\geq\Lambda_p^{\mathrm{sec}},\forall k,p, &(5c)\\ &\left|\mathbf{q}^H\mathbf{H}_p\mathbf{v}\right|^2\Big/\sigma_p^2\leq I_{th},\forall p, &(5d)\\ &\left|[\mathbf{q}]_n\right|=1,\forall n\in\{1,\cdots,N+1\}=\mathbb{N}, &(5e)\end{aligned}$$

where Λ_s and Λ_p^{sec} are the QoS and SR requirement of SU and the *p*th PU, respectively. I_{th} is the interference threshold for PUs. $[\mathbf{q}]_n$ stands for the *n*th element of $\mathbf{q}$. Obviously, as the result of the coupling of $\mathbf{q}$ and $\mathbf{w}_p\left(\mathbf{v}\right)$, problem (5) is non-convex. In what follows, we will present an efficient alternating algorithm to find the optimal solution.

III. Proposed Alternating Algorithm

An efficient alternating optimization algorithm is proposed in this section to solve $\mathbf{q}$ and $\mathbf{w}_p\left(\mathbf{v}\right)$ alternatively. We first transform PUs' SR constraint into a SOC form.

Denote $\mathbf{F}_v=\mathbf{f}_v\mathbf{f}_v^H\ (v\in\{s,p,\{e,k\}\})$, $\mathbf{W}_p=\mathbf{w}_p\mathbf{w}_p^H$, $\mathbf{V}=\mathbf{v}\mathbf{v}^H$, $\mathbf{\Theta}=\mathbf{q}\mathbf{q}^H$, $\mathbf{\Sigma}_p=\sum_{i=1,i\neq p}^{P}\mathbf{W}_i$. Then, by substituting (3) and (4) into (5), (5) can be recast to

$$\begin{aligned}\min_{\mathbf{W}_p,\mathbf{V},\mathbf{\Theta}}\quad&\sum_{p=1}^{P}\mathrm{tr}\left(\mathbf{W}_p\right)+\mathrm{tr}\left(\mathbf{V}\right) &(6a)\\ \text{s.t.}\quad&1+\frac{\mathrm{tr}\left(\mathbf{H}_s^H\mathbf{\Theta}\mathbf{H}_s\mathbf{V}\right)}{\sum_{p=1}^{P}\mathrm{tr}\left(\mathbf{F}_s\mathbf{W}_p\right)+\sigma_s^2}\geq2^{\Lambda_s}, &(6b)\\ &\frac{1+\frac{\mathrm{tr}\left(\mathbf{F}_p\mathbf{W}_p\right)}{\mathrm{tr}\left(\mathbf{F}_p\mathbf{\Sigma}_p\right)+\mathrm{tr}\left(\mathbf{H}_p^H\mathbf{\Theta}\mathbf{H}_p\mathbf{V}\right)+\sigma_p^2}}{1+\frac{\mathrm{tr}\left(\mathbf{F}_{e,k}\mathbf{W}_p\right)}{\mathrm{tr}\left(\mathbf{F}_{e,k}\mathbf{\Sigma}_p\right)+\mathrm{tr}\left(\mathbf{H}_{e,k}^H\mathbf{\Theta}\mathbf{H}_{e,k}\mathbf{V}\right)+\sigma_{e,k}^2}}\geq2^{\Lambda_p^{\mathrm{sec}}},\forall k,p, &(6c)\\ &\mathrm{tr}\left(\mathbf{H}_p^H\mathbf{\Theta}\mathbf{H}_p\mathbf{V}\right)\leq\sigma_p^2I_{th},\forall p, &(6d)\\ &\left[\mathbf{\Theta}\right]_{n,n}=1,\forall n\in\{1,\cdots,N+1\}=\mathbb{N}, &(6e)\\ &\mathrm{rank}\left(\mathbf{\Theta}\right)=1,\mathrm{rank}\left(\mathbf{V}\right)=1,\mathrm{rank}\left(\mathbf{W}_p\right)=1,\forall p. &(6f)\end{aligned}$$

Obviously, the constraints (6b)–(6c) can be, respectively, rewritten as

$$\mathrm{tr}\left(\mathbf{H}_s^H\mathbf{\Theta}\mathbf{H}_s\mathbf{V}\right)-a_s\sum_{p=1}^{P}\mathrm{tr}\left(\mathbf{F}_s\mathbf{W}_p\right)\geq a_s\sigma_s^2, \tag{7}$$

$$\begin{aligned}&\frac{\mathrm{tr}\left(\mathbf{F}_p\mathbf{W}_p\right)+\mathrm{tr}\left(\mathbf{F}_p\mathbf{\Sigma}_p\right)+\mathrm{tr}\left(\mathbf{H}_p^H\mathbf{\Theta}\mathbf{H}_p\mathbf{V}\right)+\sigma_p^2}{\mathrm{tr}\left(\mathbf{F}_p\mathbf{\Sigma}_p\right)+\mathrm{tr}\left(\mathbf{H}_p^H\mathbf{\Theta}\mathbf{H}_p\mathbf{V}\right)+\sigma_p^2}\\ &\times\frac{\mathrm{tr}\left(\mathbf{F}_{e,k}\mathbf{\Sigma}_p\right)+\mathrm{tr}\left(\mathbf{H}_{e,k}^H\mathbf{\Theta}\mathbf{H}_{e,k}\mathbf{V}\right)+\sigma_{e,k}^2}{\mathrm{tr}\left(\mathbf{F}_{e,k}\mathbf{W}_p\right)+\mathrm{tr}\left(\mathbf{F}_{e,k}\mathbf{\Sigma}_p\right)+\mathrm{tr}\left(\mathbf{H}_{e,k}^H\mathbf{\Theta}\mathbf{H}_{e,k}\mathbf{V}\right)+\sigma_{e,k}^2}\\ &\geq2^{\Lambda_p^{\mathrm{sec}}},\forall k,p,\end{aligned} \tag{8}$$

where $a_s=2^{\Lambda_s}-1$.

Proposition 1: By assuming $\frac{A+B}{B}\frac{C}{D+C}\geq E$, we will have $\left[A+\left(1-E\right)B\right]\left[C+\frac{E}{E-1}D\right]\geq\frac{E}{E-1}AD$.

Proof:

$$\begin{aligned}&\frac{A+B}{B}\frac{C}{D+C}\geq E\Leftrightarrow\left(A+B\right)C\geq EB\left(D+C\right)\\ &\Leftrightarrow\left(A+B\right)C+\frac{E}{E-1}AD-EB\left(D+C\right)\geq\frac{E}{E-1}AD\\ &\Leftrightarrow\left(A+B-EB\right)C+\frac{E}{E-1}AD-EBD\geq\frac{E}{E-1}AD\\ &\Leftrightarrow\left[A+\left(1-E\right)B\right]C+\frac{E}{E-1}AD-EBD\geq\frac{E}{E-1}AD\\ &\Leftrightarrow\left[A+\left(1-E\right)B\right]\left[C+\frac{E}{E-1}D\right]\geq\frac{E}{E-1}AD.\end{aligned} \tag{9}$$

By substituting $A=\mathrm{tr}\left(\mathbf{F}_p\mathbf{W}_p\right)$, $B=\mathrm{tr}\left(\mathbf{F}_p\mathbf{\Sigma}_p\right)+\mathrm{tr}\left(\mathbf{H}_p^H\mathbf{\Theta}\mathbf{H}_p\mathbf{V}\right)+\sigma_p^2$, $C=\mathrm{tr}\left(\mathbf{F}_{e,k}\mathbf{\Sigma}_p\right)+\mathrm{tr}\left(\mathbf{H}_{e,k}^H\mathbf{\Theta}\mathbf{H}_{e,k}\mathbf{V}\right)+\sigma_{e,k}^2$, $D=\mathrm{tr}\left(\mathbf{F}_{e,k}\mathbf{W}_p\right)$, $E=2^{\Lambda_p^{\mathrm{sec}}}$ into the *Proposition 1*, (8) can be further expressed as (10). In addition, the right side of (10) can be recast to

$$\begin{aligned}&\mathrm{tr}\left(\mathbf{F}_p\mathbf{W}_p\right)\mathrm{tr}\left(\mathbf{F}_{e,k}\mathbf{W}_p\right)\\ &\overset{a}{=}\left[vec\left(\mathbf{W}_p^T\right)\right]^Tvec\left(\mathbf{F}_p\right)\left[vec\left(\mathbf{F}_{e,k}^T\right)\right]^Tvec\left(\mathbf{W}_p\right)\\ &\overset{b}{=}\left[vec\left(\mathbf{W}_p^T\right)\right]^T\left[\left(\mathbf{f}_{e,k}\mathbf{f}_p^H\right)^T\otimes\left(\mathbf{f}_p\mathbf{f}_{e,k}^H\right)\right]vec\left(\mathbf{W}_p\right)\\ &=\left[vec\left(\mathbf{W}_p^T\right)\right]^T\left[\left(\mathbf{f}_{e,k}\mathbf{f}_p^H\right)^T\otimes\left(\mathbf{f}_{e,k}\mathbf{f}_p^H\right)^H\right]vec\left(\mathbf{W}_p\right)\\ &\overset{c}{=}\mathrm{tr}\left[\left(\mathbf{f}_{e,k}\mathbf{f}_p^H\right)^H\mathbf{W}_p\left(\mathbf{f}_{e,k}\mathbf{f}_p^H\right)\mathbf{W}_p\right]\\ &\overset{d}{=}\left[\mathrm{tr}\left(\mathbf{G}_{k,p}\mathbf{W}_p\right)\right]^2,\end{aligned} \tag{11}$$

where $\mathbf{G}_{k,p}=\mathbf{f}_{e,k}\mathbf{f}_p^H$. The above equation (11a) is obtained by $\mathrm{tr}\left(\mathbf{A}^T\mathbf{B}\right)=\left[vec\left(\mathbf{A}\right)\right]^Tvec\left(\mathbf{B}\right)$, where $\mathbf{A}$ and $\mathbf{B}$ are $m\times n$ matrices. For $\mathbf{A}_{m\times n}$, $\mathbf{B}_{n\times k}$, $\mathbf{C}_{1\times p}$, $\mathbf{D}_{p\times q}$ and $\mathbf{a}_{m\times1}$, $\mathbf{b}_{n\times1}$,

$vec\left(\mathbf{ab}^T\right) = \mathbf{b}\otimes\mathbf{a}$ and $(\mathbf{A}\otimes\mathbf{C})(\mathbf{B}\otimes\mathbf{D}) = \mathbf{AB}\otimes\mathbf{CD}$ can be derived. Thus, we have (11b). Equation (11c) comes from $\mathrm{tr}(\mathbf{ABCD}) = \left(vec\left(\mathbf{D}^T\right)\right)^T\left(\mathbf{C}^T\otimes\mathbf{A}\right)vec(\mathbf{B})$. For a rank-1 matrix $\mathbf{A}$, we can obtain $\mathrm{tr}\left(\mathbf{A}^2\right) = [\mathrm{tr}(\mathbf{A})]^2$, which results in (11d). By substituting (11) into (10), we can attain

$$\frac{1}{4}\left[(X+Y)^2-(X-Y)^2\right] \geq \left[\sqrt{\frac{2^{\Lambda_p^{\mathrm{sec}}}}{2^{\Lambda_p^{\mathrm{sec}}}-1}}\mathrm{tr}\left(\mathbf{G}_{k,p}\mathbf{W}_p\right)\right]^2, \tag{12}$$

which can be rewritten in another form, given by

$$\left\|\begin{bmatrix}\sqrt{\frac{2^{\Lambda_p^{\mathrm{sec}}}}{2^{\Lambda_p^{\mathrm{sec}}}-1}}\mathrm{tr}\left(\mathbf{G}_{k,p}\mathbf{W}_p\right)\\ \frac{1}{2}(X-Y)\end{bmatrix}\right\| \leq \frac{1}{2}(X+Y), \tag{13}$$

where

$$\begin{aligned} X =& \mathrm{tr}\left(\mathbf{F}_p\mathbf{W}_p\right) + \left(1-2^{\Lambda_p^{\mathrm{sec}}}\right) \\ & \times\left(\mathrm{tr}\left(\mathbf{F}_p\mathbf{\Sigma}_p\right)+\mathrm{tr}\left(\mathbf{H}_p^H\mathbf{\Theta}\mathbf{H}_p\mathbf{V}\right)+\sigma_p^2\right), \\ Y =& \mathrm{tr}\left(\mathbf{F}_{e,k}\mathbf{\Sigma}_p\right)+\mathrm{tr}\left(\mathbf{H}_{e,k}^H\mathbf{\Theta}\mathbf{H}_{e,k}\mathbf{V}\right)+\sigma_{e,k}^2 \\ & + \frac{2^{\Lambda_p^{\mathrm{sec}}}}{2^{\Lambda_p^{\mathrm{sec}}}-1}\mathrm{tr}\left(\mathbf{F}_{e,k}\mathbf{W}_p\right). \end{aligned} \tag{14}$$

Consequently, problem (6) can be recast to

$$\min_{\mathbf{W}_p,\mathbf{V},\mathbf{\Theta}} \quad \sum_{p=1}^{P}\mathrm{tr}\left(\mathbf{W}_p\right)+\mathrm{tr}\left(\mathbf{V}\right) \tag{15a}$$

$$\text{s.t.} \quad (6d),(6e),(6f),(7),(13). \tag{15b}$$

The coupled $\mathbf{V}$ and $\mathbf{\Theta}$ lead to the non-convexity of (15), which makes the solution process of (15) difficult. Thus, an alternating optimization algorithm will be proposed in the following. In other words, (15) will be decomposed into two sub-problems, namely, (16) under fixed $\mathbf{\Theta}$, and (22) under fixed $\mathbf{W}_p$ and $\mathbf{V}$.

A. Sub-Problem 1: Solving $\mathbf{W}_p$ and $\mathbf{V}$ Under Fixed $\mathbf{\Theta}$

Since $\mathbf{\Theta}$ is fixed, sub-problem 1 can be expressed as

$$\min_{\mathbf{W}_p,\mathbf{V}} \quad \sum_{p=1}^{P}\mathrm{tr}\left(\mathbf{W}_p\right)+\mathrm{tr}\left(\mathbf{V}\right) \tag{16a}$$

$$\text{s.t.} \quad (6d),(7),(13), \tag{16b}$$

$$\mathrm{rank}\left(\mathbf{V}\right)=1, \mathrm{rank}\left(\mathbf{W}_p\right)=1, \forall p. \tag{16c}$$

It is obvious that the constraint (16c) makes the solution process of (16) challenging. For simplicity, we denote $\mathbf{V}$ as $\mathbf{W}_0$. For addressing the rank-1 non-convex constraint, we exploit the characteristic $\mathrm{rank}(\mathbf{X})=1 \Leftrightarrow \mathrm{tr}(\mathbf{X})-\lambda_{\max}(\mathbf{X})\leq 0$ for any matrix $\mathbf{X}\succeq 0$ [44]. As such, (16) can be recast to

$$\min_{\mathbf{W}_i} \quad \sum_{i=0}^{P}\mathrm{tr}\left(\mathbf{W}_i\right) \tag{17a}$$

$$\text{s.t.} \quad (6d),(7),(13), \tag{17b}$$

$$\mathrm{tr}\left(\mathbf{W}_i\right)-\lambda_{\max}\left(\mathbf{W}_i\right)\leq 0, \forall i. \tag{17c}$$

Note that the inequality $\mathrm{tr}(\mathbf{W}_i)\geq\lambda_{\max}(\mathbf{W}_i)$ always holds for any matrix $\mathbf{W}_i\succeq 0$. As such, we aims to drive $\mathrm{tr}(\mathbf{W}_i)-\lambda_{\max}(\mathbf{W}_i)$ close to zero. Taking advantage of the penalty term manner, (17c) can be incorporated into the objective function (17a), yielding

$$\min_{\mathbf{W}_i} \quad \sum_{i=0}^{P}\mathrm{tr}\left(\mathbf{W}_i\right)+\sum_{i=0}^{P}\rho_i\left[\mathrm{tr}\left(\mathbf{W}_i\right)-\lambda_{\max}\left(\mathbf{W}_i\right)\right] \tag{18a}$$

$$\text{s.t.} \quad (6d),(7),(13), \tag{18b}$$

where the penalty factor ρ_i ought to be high enough to attain a low value of $\mathrm{tr}(\mathbf{W}_i)-\lambda_{\max}(\mathbf{W}_i)$. As we can see, (18a) is a concave function. Since $\lambda_{\max}(\mathbf{W}_i)$ is non-smooth over the domain, we make use of its sub-gradient, i.e., $\partial\lambda_{\max}(\mathbf{X}) = \mathbf{x}_{\max}\mathbf{x}_{\max}^H$, yielding [50]

$$\lambda_{\max}(\mathbf{X})-\lambda_{\max}(\mathbf{W}_i)\geq\left\langle\mathbf{w}_{i,\max}\mathbf{w}_{i,\max}^H, \mathbf{X}-\mathbf{W}_i\right\rangle, \forall\mathbf{X}\geq 0. \tag{19}$$

Next, by means of the maximum eigenvalue and corresponding unit eigenvector $\mathbf{w}_i^{(m)}$ to assign the initial matrix $\mathbf{W}_i^{(m)}$, which satisfies the constraint (18b), one can attain a second-order-cone-programming (SOCP) problem as

$$\min_{\mathbf{W}_i} \quad \sum_{i=0}^{P}\mathrm{tr}\left(\mathbf{W}_i\right)+\sum_{i=0}^{P}\rho_i\left[\mathrm{tr}\left(\mathbf{W}_i\right)-\left\langle\mathbf{w}_i^{(m)}\mathbf{w}_i^{(m)H}, \mathbf{W}_i\right\rangle\right] \tag{20a}$$

$$\text{s.t.} \quad (6d),(7),(13). \tag{20b}$$

Compared with $\mathbf{W}_i^{(m)}$, $\mathbf{W}_i^{(m+1)}$ solved from the problem (20) can produce a lower (18a). In specific, by supposing

Algorithm 1: The proposed transmit beamforming algorithm for solving sub-problem 1

Input: $\mathbf{H}$, $\mathbf{h}_v$, $\mathbf{h}_{dv}$, $\mathbf{f}_v$, $\mathbf{f}_{dv}$ $(v\in\{s,p,\{e,k\}\})$, Λ_s, Λ_p^{sec}, I_{th}

Output: Optimal transmit beamforming $\mathbf{W}_i^*$

Initialize $\rho_i=10$, $m=0$, $n=0$, $\mathbf{\Theta}$, ε;
Initialize $\mathbf{W}_i^{(0)}$ $(i=0,1\cdots,P)$ satisfying (20b);
while $\left|\mathrm{tr}\left(\mathbf{W}_i^{(m)}\right)-\lambda_{\max}\left(\mathbf{W}_i^{(m)}\right)\right|\geq\varepsilon$ **do**
  Find the optimal solution $\mathbf{W}_i^{(m+1)}$ of (20);
  if $\mathbf{W}_i^{(m+1)}\approx\mathbf{W}_i^{(m)}$ **then**
    Set $\rho_i := 2\rho_i$;
  else
    Set $m := m+1$;
    Set $\rho_i = 10$;
  end
end
Obtain ρ_i and set $\mathbf{W}_i^{(0)} := \mathbf{W}_i^{(m)}$;
repeat
  Solve (20) to obtain the solution $\mathbf{W}_i^{(n+1)}$;
  Set $n := n+1$;
until $\left|\mathrm{tr}\left(\mathbf{W}_i^{(n)}\right)-\lambda_{\max}\left(\mathbf{W}_i^{(n)}\right)\right|<\varepsilon$;
Obtain the optimal transmit beamforming $\mathbf{W}_i^* := \mathbf{W}_i^{(n)}$.

that $\mathbf{W}_i^{(m+1)}$ is the solved optimization variable of (20), one have

$$\begin{aligned}
&g\left(\mathbf{W}_i^{(m+1)}\right) = \sum_{i=0}^{P} \mathrm{tr}\left(\mathbf{W}_i^{(m+1)}\right) \\
&+ \sum_{i=0}^{P} \rho_i \left[\mathrm{tr}\left(\mathbf{W}_i^{(m+1)}\right) - \lambda_{\max}\left(\mathbf{W}_i^{(m+1)}\right)\right] \\
&\le \sum_{i=0}^{P} \mathrm{tr}\left(\mathbf{W}_i^{(m+1)}\right) + \sum_{i=0}^{P} \rho_i \left[\mathrm{tr}\left(\mathbf{W}_i^{(m+1)}\right) - \lambda_{\max}\left(\mathbf{W}_i^{(m)}\right)\right. \\
&\left. - \left\langle \mathbf{w}_i^{(m)}\mathbf{w}_i^{(m)H}, \mathbf{W}_i^{(m+1)} - \mathbf{W}_i^{(m)} \right\rangle\right] \\
&= \sum_{i=0}^{P} \mathrm{tr}\left(\mathbf{W}_i^{(m+1)}\right) + \sum_{i=0}^{P} \rho_i \left[\mathrm{tr}\left(\mathbf{W}_i^{(m+1)}\right) - \left\langle \mathbf{w}_i^{(m)}\mathbf{w}_i^{(m)H}, \right.\right. \\
&\left.\left. \mathbf{W}_i^{(m+1)} \right\rangle + \left\langle \mathbf{w}_i^{(m)}\mathbf{w}_i^{(m)H}, \mathbf{W}_i^{(m)} \right\rangle - \lambda_{\max}\left(\mathbf{W}_i^{(m)}\right)\right] \\
&\le \sum_{i=0}^{P} \mathrm{tr}\left(\mathbf{W}_i^{(m)}\right) + \sum_{i=0}^{P} \rho_i \left[\mathrm{tr}\left(\mathbf{W}_i^{(m)}\right) - \left\langle \mathbf{w}_i^{(m)}\mathbf{w}_i^{(m)H}, \right.\right. \\
&\left.\left. \mathbf{W}_i^{(m)} \right\rangle + \left\langle \mathbf{w}_i^{(m)}\mathbf{w}_i^{(m)H}, \mathbf{W}_i^{(m)} \right\rangle - \lambda_{\max}\left(\mathbf{W}_i^{(m)}\right)\right] \\
&= \sum_{i=0}^{P} \mathrm{tr}\left(\mathbf{W}_i^{(m)}\right) + \sum_{i=0}^{P} \rho_i \left[\mathrm{tr}\left(\mathbf{W}_i^{(m)}\right) - \lambda_{\max}\left(\mathbf{W}_i^{(m)}\right)\right] \\
&= g\left(\mathbf{W}_i^{(m)}\right),
\end{aligned} \tag{21}$$

which verifies the iterative procedure.

As a consequence, we summarize our proposed transmit beamforming algorithm at the CBS/PBS using SOCP together with penalty function as in Algorithm 1, which includes the choices of penalty coefficient ρ_i and initial feasible solution $\mathbf{W}_i^{(0)}$.

B. Sub-Problem 2: Solving $\mathbf{\Theta}$ Under Fixed $\mathbf{W}_p$ and $\mathbf{V}$

When $\{\mathbf{W}_p, \mathbf{V}\}$ are given, (15) will develop into a feasibility check problem, written by

$$\begin{aligned}
&\text{Find} \quad \mathbf{\Theta} && \text{(22a)}\\
&\text{s.t.} \quad (6d), (7), (13), && \text{(22b)}\\
&\qquad [\mathbf{\Theta}]_{n,n} = 1, \forall n \in \{1, \cdots, N+1\} = \mathbb{N}, && \text{(22c)}\\
&\qquad \mathrm{rank}\,(\mathbf{\Theta}) = 1. && \text{(22d)}
\end{aligned}$$

In order to obtain a better converged solution in the optimization process, we further reformulate (22) into a problem with a clear objective function. The basic principle is that for the sub-problem 1, all constraints are valid at the optimal solution. To this end, we can optimize RIS's phase shift to force SU's transmission rate and PUs' interference temperature to be greater and smaller than corresponding thresholds in (22), which can directly leads to a cut in the total transmit power of sub-problem 1. Accordingly, problem (22) can be transformed into the following form

$$\begin{aligned}
\max_{\delta_p \ge 0, \mathbf{\Theta}} \quad & \sum_{p=0}^{P} \delta_p && \text{(23a)}\\
\text{s.t.} \quad & \mathrm{tr}\left(\mathbf{H}_s^H \mathbf{\Theta} \mathbf{H}_s \mathbf{V}\right) - a_s \sum_{p=1}^{P} \mathrm{tr}\left(\mathbf{F}_s \mathbf{W}_p\right) \ge a_s \sigma_s^2 + \delta_0, && \text{(23b)}\\
& \left\| \begin{bmatrix} \sqrt{\frac{2^{\Lambda_p^{\mathrm{sec}}}}{2^{\Lambda_p^{\mathrm{sec}}}-1}}\mathrm{tr}\left(\mathbf{G}_{k,p}\mathbf{W}_p\right) \\ \frac{1}{2}\left(X - Y\right) \end{bmatrix} \right\| \le \frac{1}{2}\left(X + Y\right), \forall k, p, && \text{(23c)}\\
& \mathrm{tr}\left(\mathbf{H}_p^H \mathbf{\Theta} \mathbf{H}_p \mathbf{V}\right) + \delta_p \le \sigma_p^2 I_{th}, \forall p, && \text{(23d)}\\
& [\mathbf{\Theta}]_{n,n} = 1, \forall n \in \{1, \cdots, N+1\} = \mathbb{N}, && \text{(23e)}\\
& \mathrm{rank}\,(\mathbf{\Theta}) = 1, && \text{(23f)}
\end{aligned}$$

where δ_0 and δ_p can be explained as the "transmission rate residual" of SU and the "interference temperature residual" of the pth PU, respectively.

In a similar manner as (16), we use the penalty function to address the rank-1 non-convex constraint. Thus, by means of the maximum eigenvalue and corresponding unit eigenvector $\mathbf{q}^{(n)}$ to assign the initial matrix $\mathbf{\Theta}^{(n)}$, satisfying (23b)–(23e), (23) can be further recast to

$$\begin{aligned}
\max_{\mathbf{\Theta}} \quad & \sum_{p=0}^{P} \delta_p - \beta\left[\mathrm{tr}\left(\mathbf{\Theta}\right) - \left\langle \mathbf{q}^{(n)}\mathbf{q}^{(n)H}, \mathbf{\Theta} \right\rangle\right] && \text{(24a)}\\
\text{s.t.} \quad & (23b) - (23e), && \text{(24b)}
\end{aligned}$$

where the penalty factor β ought to be high enough to attain a low value of $\mathrm{tr}\left(\mathbf{\Theta}\right) - \lambda_{\max}\left(\mathbf{\Theta}\right)$.

Consequently, we are able to attain the optimal solution to (24) by means of CVX.

C. The Overall Algorithm

By alternatively solving problem (20) and problem (24), the total transmit power tends to monotonically decrease. Algorithm 2 shows the whole flow of the solution process.

Proposition 2: With the alternating iterations of Algorithm 2, the total transmit power of the constrained problem is non-increasing.

Proof: For the feasible solution $(\mathbf{W}_i, \mathbf{\Theta})$ of problem (15), we suppose that the total transmit power is $h\left(\mathbf{W}_i, \mathbf{\Theta}\right)$. According to line 6 of Algorithm 2, a feasible solution $\left(\mathbf{W}_i^{(j)}, \mathbf{\Theta}^{(j)}\right)$ of (24) is also the feasible solution of (20). Then, $\left(\mathbf{W}_i^{(j)}, \mathbf{\Theta}^{(j-1)}\right)$ and $\left(\mathbf{W}_i^{(j+1)}, \mathbf{\Theta}^{(j)}\right)$ in line 4 of Algorithm 2 are also feasible for (20), which follows

$$h\left(\mathbf{W}_i^{(j+1)}, \mathbf{\Theta}^{(j)}\right) \overset{(e)}{\le} h\left(\mathbf{W}_i^{(j)}, \mathbf{\Theta}^{(j)}\right) \overset{(f)}{=} h\left(\mathbf{W}_i^{(j)}, \mathbf{\Theta}^{(j-1)}\right), \tag{25}$$

where the inequality (e) holds attributing to the fact that $\mathbf{W}_i^{(j+1)}$ is the optimized transmit beamforming. The equation (f) can be interpreted as the total transmit power is only related to $\mathbf{W}_i$, and has nothing to do with $\mathbf{\Theta}$.

Algorithm 2: Alternating optimization algorithm for solving problem (15)

Input: $\mathbf{H}$, $\mathbf{h}_v$, $\mathbf{h}_{dv}$, $\mathbf{f}_v$, $\mathbf{f}_{dv}$ $(v \in \{s, p, \{e,k\}\})$, Λ_s, Λ_p^{sec}, I_{th}

Output: Optimal transmit beamforming $\mathbf{V}^*$ at the CBS, optimal reflect beamforming $\boldsymbol{\Theta}^*$ at the RIS, optimal transmit beamforming $\mathbf{W}_p^*$ at the PBS, and the minimum total transmit power $\sum_{p=1}^{P} \text{tr}\left(\mathbf{W}_p^*\right) + \text{tr}\left(\mathbf{V}^*\right)$

Initialize $j = 0$, $P_{tot}^{(0)} = 0$, $\boldsymbol{\Theta}^{(0)}$;

repeat

  Set $j := j + 1$;

  Set $\boldsymbol{\Theta}^* := \boldsymbol{\Theta}^{(j-1)}$;

  Perform **Algorithm 1** with given $\boldsymbol{\Theta}^*$ to obtain $\mathbf{W}_i^{(j)}$;

  Set $\mathbf{W}_i^* := \mathbf{W}_i^{(j)}$;

  Obtain $\boldsymbol{\Theta}^{(j)}$ by solving (24) with given $\mathbf{W}_i^*$ through a simmilar manner as the Algorithm 1;

  Update $P_{tot}^{(j)} := \sum_{i=0}^{P} \text{tr}\left(\mathbf{W}_i^{(j)}\right)$;

until $\left|P_{tot}^{(j)} - P_{tot}^{(j-1)}\right| \leq \varepsilon$;

Obtain

(i) $\mathbf{V}^* = \mathbf{W}_0^*$ at the CBS;

(ii) $\boldsymbol{\Theta}^* = \boldsymbol{\Theta}^{(j)}$ at the RIS;

(iii) $\mathbf{W}_p^*$ at the PBS.

Since the total transmit power always has a lower bound of 0, combined with the *Proposition 2*, we can show the convergence of Algorithm 2.

IV. Simulation Results

We provide simulation results in this section to verify the effectiveness of the proposed algorithm. The simulation scenario is shown in Fig. 2: The coordinates of CBS, RIS, SU and PBS are geographically (0, 0) m, (50, 30) m, (50, 0) m, and (150, 0) m. Plus, the coordinates of P PUs and K Eves are uniformly along the line from (110, 10) m to (140, 10) m, and from (70,15) m to (100,15) m. The channel coefficients are modeled by $\mathbf{h}(\mathbf{f}) = \sqrt{G_0 d^{-c}}\mathbf{g}$, where $G_0 = -30$ dB represents the path loss at the reference point [32]. $\mathbf{g}$, c, and d respectively indicate the channel fading coefficient, path loss exponent and corresponding distance. As for the setting of path loss exponents, due to the relatively large distance and random scattering of the CBS-SU, PBS-PUs and PBS-Eves channels, we set the related path loss exponent as 3. Since the RIS can be practically deployed in line-of-sight (LoS) with the CBS and SU, we set the path loss exponent of RIS-related channels as 2.2 [24]. Besides, the other parameters are set as $K = 2$, $P = 2$, $M_c = M_p = 4$, $N = 16$, $\sigma_s^2 = \sigma_p^2 = \sigma_{e,k}^2 = -90$ dBm, $I_{th} = 10$ dB, and $\varepsilon = 10^{-3}$,

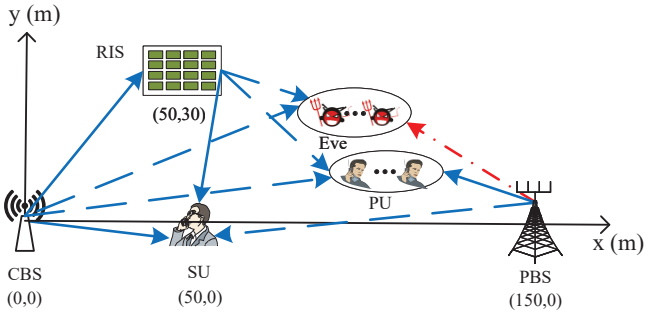

Fig. 2. The simulation scenario.

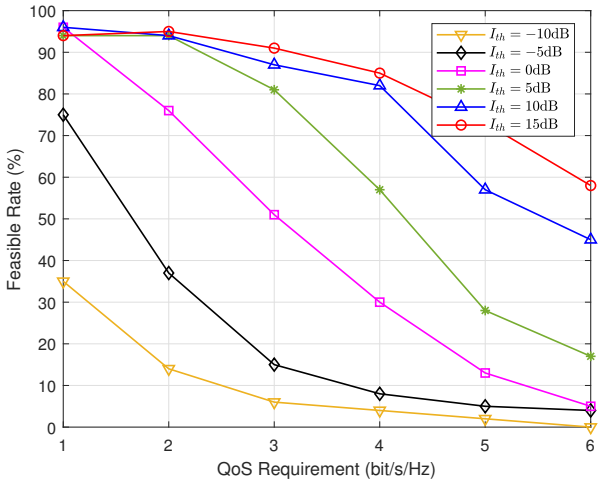

Fig. 3. Feasibility of the proposed algorithm.

unless otherwise stated. Without loss of generality, we set $\Lambda_p^{\text{sec}} = \Lambda_{\text{sec}}, \forall p$.

We also compare the results with other benchmarks: 1) Optimized CBS maximum ratio transmission (MRT) algorithm: It performs the MRT at the CBS, namely, $\mathbf{v} = \sqrt{P_c}\frac{\mathbf{H}^H\mathbf{Q}^H\mathbf{h}_s + \mathbf{h}_{ds}}{\|\mathbf{H}^H\mathbf{Q}^H\mathbf{h}_s + \mathbf{h}_{ds}\|}$, where P_c is the power allocated to SU. The transmit beamforming $\mathbf{w}_p$ at the PBS and phase shift matrix $\mathbf{Q}$ of the RIS are obtained by using the proposed algorithm; 2) PBS zero-forcing (ZF) algorithm: It can be used to enhance the signals from PBS to PUs while nulling the signals to the Eves [51]. Specifically, it maximizes $\left|\mathbf{f}_p^T\tilde{\mathbf{w}}_p\right|^2$ under the constraints $\mathbf{f}_p^T\tilde{\mathbf{w}}_j = 0\,(j \neq p)$, $\mathbf{f}_{e,k}^T\tilde{\mathbf{w}}_p = 0$ and $\tilde{\mathbf{w}}_p^H\tilde{\mathbf{w}}_p = 1$. Then, by substituting $\mathbf{w}_p = \sqrt{P_p}\tilde{\mathbf{w}}_p$ into the power minimization problem (P_p is the power allocated to the pth PU), the transmit beamforming $\mathbf{v}$ at the CBS and phase shift matrix $\mathbf{Q}$ of the RIS can be obtained by using the proposed algorithm; 3) Proposed algorithm (No RIS): The transmit beamforming $\mathbf{v}$ at the CBS and the transmit beamforming $\mathbf{w}_p$ at the PBS are obtained by using the proposed algorithm, corresponding to the sub-problem 1. The simulation results are obtained by performing 1000 channel realizations.

Fig. 3 shows the feasibility rate of our proposed algorithm with $\Lambda_{sec} = 4$ bit/s/Hz. As we can see, the feasibility rate decreases with the growth of SU's QoS requirement Λ_s. In

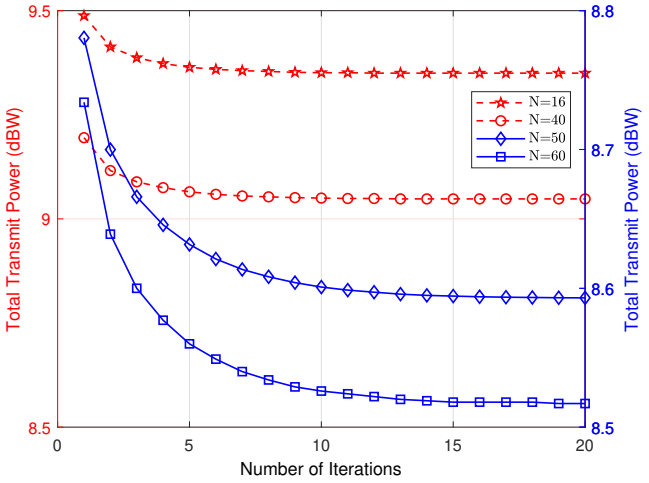

Fig. 4. Convergence of the proposed algorithm.

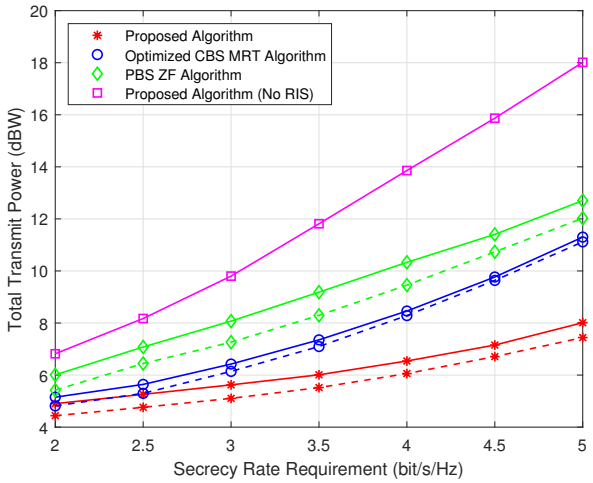

Fig. 5. Total transmit power versus PUs' SR requirement Λ_{sec}.

addition, with a given Λ_s, the decrease of PUs' interference threshold I_{th} will reduce the feasibility rate. These are due to the fact that larger Λ_s makes it difficult to satisfy SU's QoS constraint or smaller I_{th} makes PUs' limited interference constraint more stringent, thereby resulting in the decrease of feasibility rate. Another interesting phenomenon is that the feasibility rate decrease rapidly with SU's QoS requirement Λ_s at a low level of PUs' interference threshold ($I_{th} \leq 0$ dB). Hence, we cannot guarantee that SU achieves a high QoS requirement and PUs receive little interference temperature simultaneously. The value of I_{th} greater than 0 dB allows the feasibility rate to maintain a stable high value in a wide range of SU's QoS requirement Λ_s.

Fig. 4 illustrates the convergence of the proposed algorithm with $\Lambda_s = \Lambda_{sec} = 4$ bit/s/Hz. In order to make the convergence trend more obvious, the red curves and blue curves are respectively on the basis of left and right ordinate scales. As we can see, the total transmit power decreases with the iteration number, and finally reaches a stable value. It is shown that the total transmit power achieves convergence within 20 iterations, and 10 iteration rounds are enough to make the transmit power acceptable. Furthermore, we can find that larger RIS elements can bring a smaller converged transmit power value. This is because that with a larger value N, RIS has a greater degree of freedom to better increase the signal strength in the expected direction, thereby reducing the total transmit power. However, with the growth of N, more optimization variables are required to be solved, which results in a heavier computation burden, making the convergence speed slower.

Fig. 5 depicts the total transmit power versus PUs' SR requirement Λ_{sec} with $\Lambda_s = 3$ bit/s/Hz, where the solid lines and dotted lines indicate $N = 16$ and $N = 60$, respectively. The total transmit power is reduced as the number of RIS elements increases. This is because that a larger number of RIS elements N allows for more flexibility in the beamforming design, which enlarges the optimization search space, thereby reducing the total transmit power. As we can see, the total transmit power increases monotonically with the SR requirement of PUs for all algorithms, which can be explained that more transmit power is needed to meet the higher SR requirement of PUs. Moreover, we can find that the proposed algorithm saves some power compared with the proposed algorithm without RIS, and as the SR requirement of the PUs increases, the more power is saved, which verifies that the RIS in the CNR can not only be used to satisfy the QoS requirement of SU, but also be exploited as a green interference to deteriorate the wiretap channel to enhance the secure communication in the PN. Besides, in the RIS-assisted network, as for the PBS ZF algorithm, since it strictly requires that the signal sent to the pth PU will not leak any to the other PUs and all Eves, the power consumed by this algorithm is relatively large. Compared with the optimized CBS MRT algorithm, our proposed algorithm requires lower transmit power, which owes to the fact that compared with the optimized CBS MRT algorithm in which the signal is transmitted on the orthogonal complement subspace, our proposed algorithm demonstrates strong advantage in terms of transmit power, which indicates the effectiveness of our joint beamforming design by fully utilizing the channels of SU, PUs, and Eves.

Fig. 6 shows the total transmit power versus SU's QoS requirement Λ_s with $\Lambda_{sec} = 4$ bit/s/Hz, where the solid lines and dotted lines indicate $N = 16$ and $N = 60$, respectively. Similar to Fig. 5, a larger number of RIS elements can bring a lower total transmit power, which owes to the greater degree of freedom to optimize. It can be seen that with the increase of SU's QoS requirement Λ_s, the consumed power of all algorithms also increases. Also, we can find that the power budget of the proposed algorithm is the lowest among all these benchmarks, validating the superiority of our proposed algorithm. In addition, we can find that when SU's QoS requirement Λ_s is 1 bit/s/Hz, the power of our proposed algorithm without RIS is lower than that of the PBS ZF algorithm. This can be explained that the small value of SU's QoS requirement enables the proposed algorithm without RIS to meet SU's QoS requirement with relatively small power

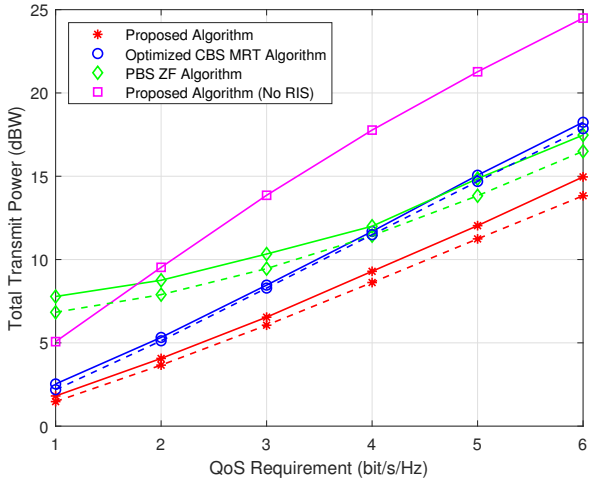

Fig. 6. Total transmit power versus SU's QoS requirement Λ_s.

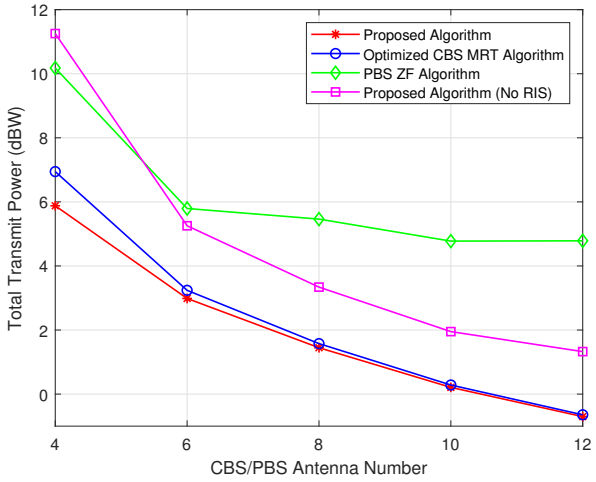

Fig. 7. Total transmit power versus the number of CBS/PBS antennas.

comsumption, while the PBS of the PBS ZF algorithm needs to suppress the leakage to mismatched PUs and all Eves, which will bring additional power consumption. When SU's QoS requirement Λ_s further increases, the role of RIS will gradually manifest. Thus, the PBS ZF algorithm consumes less power than the proposed algorithm without RIS. Furthermore, it is interesting to observe that when SU's QoS requirement Λ_s does not exceed 4bit/s/Hz, the power consumed by the optimized CBS MRT algorithm is lower than that consumed by the PBS ZF algorithm. However, when SU's QoS requirement Λ_s is no less than 5 bit/s/Hz, the optimized CBS MRT algorithm consumes more power than the PBS ZF algorithm. This is because that the optimized CBS MRT algorithm does not optimize the transmit beamforming at the CBS, which makes it consume more additional power when SU's QoS requirement Λ_s is large enough. In this case, compared with the additional power consumption caused by the unoptimized transmit beamforming at the PBS of the PBS ZF algorithm, the additional power consumption caused by the unoptimized transmit beamforming at the CBS of the optimized CBS MRT algorithm is greater.

Fig. 7 demonstrates the total transmit power versus the number of CBS/PBS antennas where $\Lambda_s = \Lambda_{sec} = 3$ bit/s/Hz. As we can see, using more CBS/PBS antennas is conductive to saving total transmit power, which is particularly obvious for the increase from 4 to 6. Nevertheless, as the number of CBS/PBS antennas further increases, the obtained power performance gain will become small. No matter how many CBS/PBS antennas is adopted, our proposed algorithm is always superior to other benchmarks. In addition, we can find that when the CBS/PBS antenna number is 4, the total transmit power of the proposed algorithm without RIS is higher than that of the PBS ZF algorithm. This can be explained that compared with the additional power consumption caused by the unoptimized transmit beamforming at the PBS of the PBS ZF algorithm, the small value of CBS antenna make the proposed algorithm without RIS consume more additional power to meet SU's QoS requirement. When the CBS/PBS

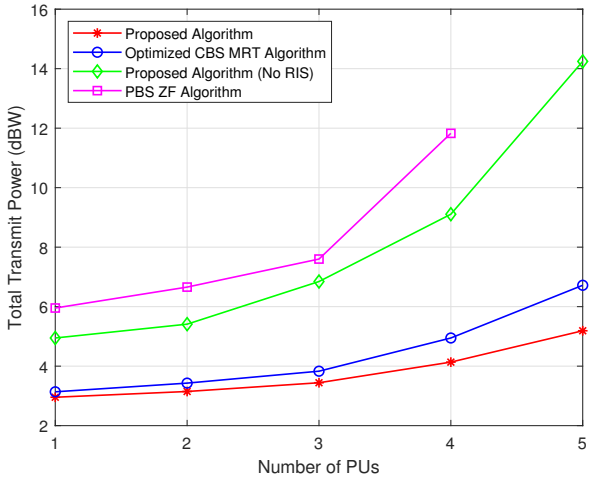

Fig. 8. Total transmit power versus the number of PUs.

antenna number is 6 or more, the PBS ZF algorithm consumes more power than the proposed algorithm without RIS. The reason is that as for the proposed algorithm without RIS, the greater number of CBS antenna can compensate for the additional power consumption caused by the loss of RIS to a certain extent, making the total transmit power less than that of the PBS ZF algorithm whose additional power consumption caused by the unoptimized transmit beamforming at the PBS. Furthermore, it can be observed that with the increase of the number of CBS/PBS antennas, the performance of the optimized CBS MRT algorithm gradually approaches that of our proposed algorithm. This can be interpreted that when the number of CBS antennas reaches a certain value, the signal strength reflected by the RIS of the optimized CBS MRT algorithm is strong enough to achieve the same effect as our proposed algorithm.

Figs. 8 and 9 respectively show the total transmit power versus the number of PUs P and the number of Eves K where $M_c = M_p = 6$, $\Lambda_s = \Lambda_{sec} = 3$ bit/s/Hz. As we

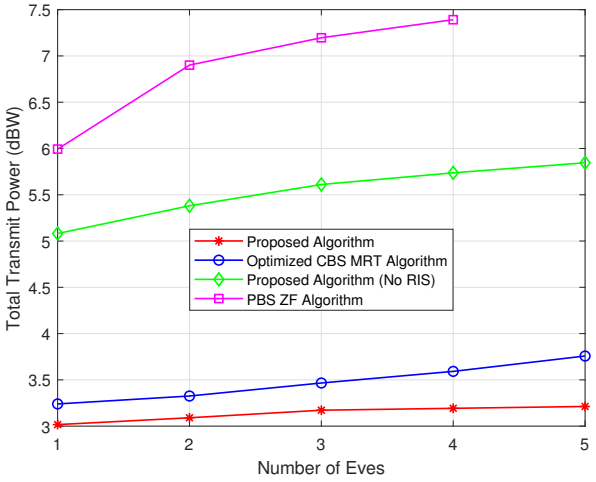

Fig. 9. Total transmit power versus the number of Eves.

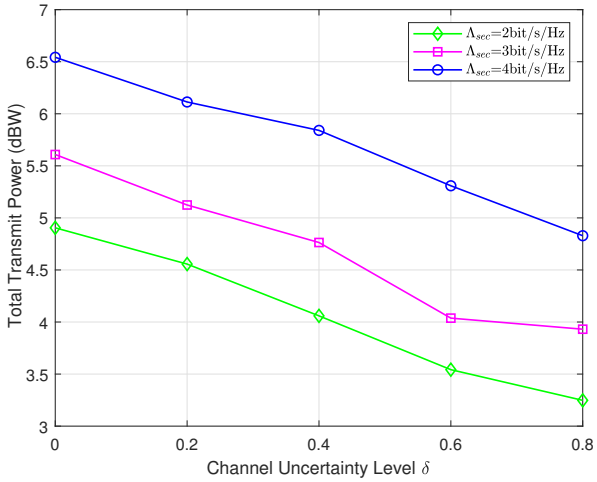

Fig. 10. Total transmit power versus channel uncertainty level δ.

can see, the total transmit power grows with the increase of the number of both PUs and Eves, since all PUs have to meet the SR requirement leaked to all Eves. Furthermore, we can find that the proposed algorithm always attains a lower total transmit power than other benchmarks. This can be explained that for PBS ZF algorithm, PBS exploits the zero points on the antenna pattern to force the signals received in the direction of mismatched PUs and all Eves to be zero. Thus, as the increase of the number of either PUs or Eves, with a limited PBS antenna number, there is almost no spatial degree-of-freedom to force the received signals in the direction of mismatched PUs and all Eves to be zero, which can account for the loss of simulation result of the PBS ZF algorithm when the number of PUs or Eves is greater than 4. Nevertheless, thanks to the joint optimization design of the SN and PN, the proposed algorithm not only takes advantage of zero points on the PBS antenna pattern, but also uses the green interference from SN to deteriorate Eves' received signals, thus the total transmit power is not very susceptible to the number of Eves and PUs. The finding is particularly beneficial to the next generation mobile communication that serves multiple users. In spite of the exploitation of joint optimization design in the proposed algorithm without RIS, the lack of RIS makes the role of green interference generated from the SN on PN not obvious, resulting in a relatively large total transmit power. Besides, although the optimized CBS MRT algorithm considers the green interference from the SN to design the transmit beamforming at the PBS, it does not take CBS's transmit beamforming into account during the optimization process, making the total transmit power a little larger than that of our proposed algorithm.

It is assumed that the exact CSI $\mathbf{h}$ of all links is not known. However, an estimation for each of them, $\bar{\mathbf{h}}$ can be obtained. The channel uncertainty model can be given by $\mathbf{h} = \bar{\mathbf{h}} + \mathbf{\Delta}$, where $\mathbf{\Delta}$ is the channel estimation error consisting of i.i.d. complex Gaussian distributed entries. To facilitate the presentation, we define the maximum normalized estimation error as $\sigma_{est}^2 = \delta / \left\| \bar{\mathbf{h}} \right\|_F$ [31]. $\delta = 0$ means that the estimated

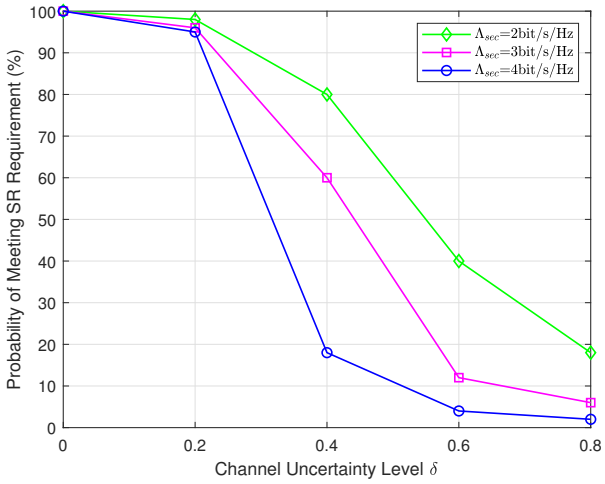

Fig. 11. Probability of meeting SR requirement versus channel uncertainty level δ.

CSI is just the perfect CSI. As we can see from Fig. 10, with the increase of channel uncertainty level, the total transmit power solved from the imperfect CSI decreases. However, this does not mean that the channel estimation error will improve the power performance. The CSI used in the solution process has errors, which makes the solved transmit power may not meet the SR constraints of PUs in the real CSI condition. As such, Fig. 11 shows the probability of meeting SR requirement versus the channel uncertainty level δ. Here, the ordinate is referred to as the probability that the PUs can meet the SR constraints in the real CSI condition when the transmit beamforming and reflect beamforming are solved from the imperfect CSI. Obviously, we can find that with the increase of channel uncertainty level, the probability of meeting SR requirement drops sharply, which means the transmit power solved from the imperfect CSI basically cannot satisfy the SR requirement in the real CSI condition.

V. Conclusion

This paper has investigated the joint beamforming design for secure communication of the SDA-based-RIS-assisted CRNs. By considering the mutual interference between the PN and SN, we have first established a constrained optimization problem to minimize the total transmit power under the premise that SU's transmission rate, PUs' SR and interference temperature meet corresponding constraints. Then, we have presented an efficient algorithm to optimize the transmit beamforming at the CBS/PBS and the reflect beamforming at the RIS alternatively. The advantage of the our proposed algorithm is that RIS not only plays the role in improving the SE of SU, but also enhances the secrecy performance of PUs by exploiting the green interference generated from the SN. Finally, computer simulation results demonstrate the effectiveness and superiority of our proposed algorithm compared with other benchmarks, and reveal that the total transmit power of our proposed algorithm is not very susceptible to the number of Eves and PUs, which is beneficial for the next generation mobile communication to serve multiple users.

References

[1] W. Zhang, C. Wang, X. Ge, and Y. Chen, "Enhanced 5G cognitive radio networks based on spectrum sharing and spectrum aggregation," *IEEE Trans. Commun.*, vol. 66, no. 12, pp. 6304–6316, Dec. 2018.

[2] C. Wang and H. Wang, "On the secrecy throughput maximization for MISO cognitive radio network in slow fading channels," *IEEE Trans. Inform. Forensics Secur.*, vol. 9, no. 11, pp. 1814–1827, Nov. 2014.

[3] D. Hamza, P. Ki-Hong, M. S. Alouini, and S. Aissa, "Throughput maximization for cognitive radio networks using active cooperation and superposition coding," *IEEE Trans. Wireless Commun.*, vol. 14, no. 6, pp. 3322–3336, Jun. 2015.

[4] M. El Tanab and W. Hamouda, "Resource allocation for underlay cognitive radio networks: A survey," *IEEE Commun. Surveys Tuts.*, vol. 19, no. 2, pp. 1249–1276, Nov. 2017.

[5] M. Bouabdellah *et al.*, "On the secrecy analysis of dual-hop underlay multi-source CRNs with multi-eavesdroppers and a multi-antenna destination," in *Proc. IEEE CommNet*, 2019.

[6] A. D.Wyner, "The wire-tap channel," *Bell Syst. Technol. J.*, vol. 54, no. 8, pp. 1355–1387, 1975.

[7] V.-D. Nguyen, T. Q. Duong, O. A. Dobre, and O.-S. Shin, "Joint information and jamming beamforming for secrecy rate maximization in cognitive radio networks," *IEEE Trans. Inform. Forensics Secur.*, vol. 11, no. 11, pp. 2609–2633, Nov. 2016.

[8] F. Gabry *et al.*, "Cooperation for secure broadcasting in cognitive radio networks," in *Proc. IEEE ICC*, 2012.

[9] A. Papadopoulos, N. D. Chatzidiamantis, and L. Georgiadis, "Network coding techniques for primary-secondary user cooperation in cognitive radio networks," *IEEE Trans. Wireless Commun.*, vol. 19, no. 6, pp. 4195–4208, Jun. 2020.

[10] Y. Y. He, J. Evans, and S. Dey, "Secrecy rate maximization for cooperative overlay cognitive radio networks with artificial noise," in *Proc. IEEE ICC*, 2014.

[11] V. Nguyen, T. M. Hoang, and O. Shin, "Secrecy capacity of the primary system in a cognitive radio network," *IEEE Trans. Veh. Technol.*, vol. 64, no. 8, pp. 3834–3843, Aug. 2015.

[12] V. Nguyen, T. Q. Duong, O. Shin, A. Nallanathan, and G. K. Karagiannidis, "Enhancing PHY security of cooperative cognitive radio multicast communications," *IEEE Trans. Cogn. Commun. Netw.*, vol. 3, no. 4, pp. 599–613, Dec. 2017.

[13] P. X. Nguyen, H. V. Nguyen, V. Nguyen, and O. Shin, "UAV-enabled jamming noise for achieving secure communications in cognitive radio networks," in *Proc IEEE CCNC*, 2019.

[14] X. He, X. Li, H. Ji, and H. Zhang, "Resource allocation for secrecy rate optimization in UAV-assisted cognitive radio network," in *Proc. IEEE WCNC*, 2021.

[15] Y. Wang *et al.*, "Resource allocation and trajectory design in UAV-assisted jamming wideband cognitive radio networks," *IEEE Trans. Cogn. Commun. Netw.*, vol. 7, no. 2, pp. 635–647, Jun. 2021.

[16] K. Lee, O. Simeone, C. B. Chae, and J. Kang, "Spectrum leasing via cooperation for enhanced physical-layer secrecy," *IEEE Trans. Veh. Technol.*, vol. 62, no. 9, pp. 4672–4678, Jun. 2013.

[17] D. Xu and Q. Li, "Resource allocation for cognitive radio with primary user secrecy outage constraint," *IEEE Syst. J.*, vol. 12, no. 1, pp. 893–904, Mar. 2018.

[18] X. Liu *et al.*, "Energy efficiency of secure cognitive radio networks with cooperative spectrum sharing," *IEEE Trans. Mobile Comput.*, vol. 18, no. 2, pp. 305–318, Feb. 2019.

[19] Q. Wu and R. Zhang, "Towards smart and reconfigurable environment: Intelligent reflecting surface aided wireless networks," *IEEE Commun. Mag.*, vol. 58, no. 1, pp. 106–112, Jan. 2020.

[20] Z. Zhang *et al.*, "Securing NOMA networks by exploiting intelligent reflecting surface," *IEEE Trans. Commun.*, vol. 70, no. 2, pp. 1096–1111, Feb. 2022.

[21] Q. Wu, S. Zhang, B. Zheng, C. You, and R. Zhang, "Intelligent reflecting surface-aided wireless communications: A tutorial," *IEEE Trans. Commun.*, vol. 69, no. 5, pp. 3313–3351, May 2021.

[22] Y. Han, W. Tang, S. Jin, C. Wen, and X. Ma, "Large intelligent surface-assisted wireless communication exploiting statistical CSI," *IEEE Trans. Veh. Technol.*, vol. 68, no. 8, pp. 8238–8242, Aug. 2019.

[23] C. Huang, A. Zappone, G. C. Alexandropoulos, M. Debbah, and C. Yuen, "Reconfigurable intelligent surfaces for energy efficiency in wireless communication," *IEEE Trans. Wireless Commun.*, vol. 18, no. 8, pp. 4157–4170, Aug. 2019.

[24] Q. Wu and R. Zhang, "Intelligent reflecting surface enhanced wireless network via joint active and passive beamforming," *IEEE Trans. Wireless Commun.*, vol. 18, no. 11, pp. 5394–5409, Nov. 2019.

[25] P. Wang, J. Fang, L. Dai, and H. Li, "Joint transceiver and large intelligent surface design for massive MIMO mmWave systems," *IEEE Trans. Wireless Commun.*, vol. 20, no. 2, pp. 1052–1064, Feb. 2021.

[26] P. Wang, J. Fang, X. Yuan, Z. Chen, and H. Li, "Intelligent reflecting surface-assisted millimeter wave communications: Joint active and passive precoding design," *IEEE Trans. Veh. Technol.*, vol. 69, no. 12, pp. 14960–14973, Dec. 2020.

[27] C. Pan *et al.*, "Multicell MIMO communications relying on intelligent reflecting surfaces," *IEEE Trans. Wireless Commun.*, vol. 19, no. 8, pp. 5218–5233, Aug. 2020.

[28] H. Guo, Y. Liang, J. Chen, and E. G. Larsson, "Weighted sum rate maximization for reconfigurable intelligent surface aided wireless networks," *IEEE Trans. Wireless Commun.*, vol. 19, no. 5, pp. 3064–3076, May 2020.

[29] M. Cui, G. Zhang, and R. Zhang, "Secure wireless communication via intelligent reflecting surface," *IEEE Wireless Commun. Lett.*, vol. 8, no. 5, pp. 1410–1414, Oct. 2019.

[30] H. Shen, W. Xu, S. Gong, Z. He, and C. Zhao, "Secrecy rate maximization for intelligent reflecting surface assisted multi-antenna communications," *IEEE Commun. Lett.*, vol. 23, no. 9, pp. 1488–1492, Sep. 2019.

[31] X. Yu, D. Xu, Y. Sun, D. W. K. Ng, and R. Schober, "Robust and secure wireless communications via intelligent reflecting surfaces," *IEEE J. Sel. Areas Commun.*, vol. 38, no. 11, pp. 2637–2652, Nov. 2020.

[32] S. Hong, C. Pan, H. Ren, K. Wang, and A. Nallanathan, "Artificial-noise-aided secure MIMO wireless communications via intelligent reflecting surface," *IEEE Trans. Commun.*, vol. 68, no. 12, pp. 7851–7866, Dec. 2020.

[33] L. Dong and H. Wang, "Secure MIMO transmission via intelligent reflecting surface," *IEEE Wireless Commun. Lett.*, vol. 9, no. 6, pp. 787–790, Jun. 2020.

[34] L. Dong and H. Wang, "Enhancing secure MIMO transmission via intelligent reflecting surface," *IEEE Trans. Wireless Commun.*, vol. 19, no. 11, pp. 7543–7556, Nov. 2020.

[35] S. Hong *et al.*, "Robust transmission design for intelligent reflecting surface-aided secure communication systems with imperfect cascaded CSI," *IEEE Trans. Wireless Commun.*, vol. 20, no. 4, pp. 2487–2501, Apr. 2021.

[36] B. Feng, Y. Wu, and M. Zheng, "Secure transmission strategy for intelligent reflecting surface enhanced wireless system," in *Proc. IEEE WCSP*, 2019.
[37] Q. Wu and R. Zhang, "Beamforming optimization for wireless network aided by intelligent reflecting surface with discrete phase shifts," *IEEE Trans. Commun.*, vol. 68, no. 3, pp. 1838–1851, Mar. 2020.
[38] Q. Wang, F. Zhou, R. Q. Hu, and Y. Qian, "Energy efficient robust beamforming and cooperative jamming design for RIS-assisted MISO networks," *IEEE Trans. Wireless Commun.*, vol. 20, no. 4, pp. 2592–2607, Apr. 2021.
[39] J. He, K. Yu, Y. Zhou, and Y. Shi, "Reconfigurable intelligent surface enhanced cognitive radio networks," in *Proc. IEEE VTC*, 2020.
[40] L. Zhang *et al.*, "Robust beamforming optimization for intelligent reflecting surface aided cognitive radio networks," in *Proc. IEEE GLOBECOM*, 2020.
[41] L. Zhang *et al.*, "Intelligent reflecting surface aided MIMO cognitive radio systems," *IEEE Trans. Veh. Technol.*, vol. 69, no. 10, pp. 11445–11457, Oct. 2020.
[42] X. Guan, Q. Wu, and R. Zhang, "Joint power control and passive beamforming in RIS-assisted spectrum sharing," *IEEE Commun. Lett.*, vol. 24, no. 7, pp. 1553–1557, Jul. 2020.
[43] J. Yuan, Y. -C. Liang, J. Joung, G. Feng, and E. G. Larsson, "Intelligent reflecting surface-assisted cognitive radio system," *IEEE Trans. Commun.*, vol. 69, no. 1, pp. 675–687, Jan. 2021.
[44] X. Wu *et al.*, "Secure and energy efficient transmission for IRS-assisted cognitive radio networks," *IEEE Trans. Cogn. Commun. Netw.*, vol. 8, no. 1, pp. 170—185, Mar. 2022.
[45] X. Wu, J. Ma, C. Gu, X. Xue, and X. Zeng, "Robust secure transmission design for IRS-assisted mmWave cognitive radio networks," *IEEE Trans. Veh. Technol.*, vol. 71, no. 8, pp. 8441–8456, Aug. 2022.
[46] L. Dong, H.-M. Wang, and H. Xiao, "Secure cognitive radio communication via intelligent reflecting surface," *IEEE Trans. Commun.*, vol. 69, no. 7, pp. 4678–4690, Jul. 2021.
[47] A. Mukherjee, S. A. A. Fakoorian, J. Huang, and A. L. Swindlehurst, "Principles of physical layer security in multiuser wireless networks: A survey," *IEEE Commun. Surveys Tuts.*, vol. 16, no. 3, pp. 1550–1573, 2014.
[48] Y. Yang, B. Zheng, S. Zhang and R. Zhang, "Intelligent reflecting surface meets OFDM: Protocol design and rate maximization," *IEEE Trans. Commun.*, vol. 68, no. 7, pp. 4522–4535, Jul. 2020.
[49] B. Zheng and R. Zhang, "Intelligent reflecting surface-enhanced OFDM: Channel estimation and reflection optimization," *IEEE Wireless Commun. Lett.*, vol. 9, no. 4, pp. 518–522, Apr. 2020.
[50] J. Hiriart-Urruty and C. Lemarechal, *Convex Analysis and Minimization Algorithms I: Fundamentals*. New York, NY, USA: Springer, 1996.
[51] Z. Ding, K. K. Leung, D. L. Goeckel, and D. Towsley, "On the application of cooperative transmission to secrecy communications," *IEEE J. Sel. Areas Commun.*, vol. 30, no. 2, pp. 359–368, Feb. 2012.

Xuewen Wu (Graduate Student Member, IEEE) received the B.S. degree from College of Computer Science and Technology, Nanjing Tech University, Nanjing, China, in 2017, and the M.S. degree from Nanjing University of Posts and Telecommunications in 2020. She is currently working towards the Ph.D. degree in Information and Communication Engineering from Tongji University. Her research interests include intelligent reflecting surface, cognitive radio, convex optimization, and physical layer security.

Jingxiao Ma received the B.Eng. degree from the University of Birmingham, U.K., in 2011, the M.Sc. degree in Wireless Communications from the University of Southampton, U.K., in 2012, and the Ph.D. degree from the University of Sheffield, in 2018. He is currently working with the College of Electronics and Information Engineering, Tongji University, where he is focusing on the areas of relay beamforming, massive MIMO systems, and cognitive radio networks.

Xiaoping Xue (Member, IEEE) received the B.S. degree in Wired Communication from Tongji University (formerly Shanghai Railway University), Shanghai, China, in 1987, and the Ph.D. degree in Communication and Information Systems from Beijing Jiaotong University, Beijing, China, in 2009. He is currently a Professor and the Director of the Department of Information and Communication Engineering, Tongji University. His research interests include secure broadband wireless communication theory under high-speed moving conditions, safe computing theory and methods, formal software and security evaluation theory and methods, and security and privacy in vehicular networks.